

See discussions, stats, and author profiles for this publication at: <https://www.researchgate.net/publication/263962120>

Removal of High-Concentration C.I. Acid Orange 7 from Aqueous Solution by Zerovalent Iron/Copper (Fe/Cu) Bimetallic Particles

ARTICLE in INDUSTRIAL & ENGINEERING CHEMISTRY RESEARCH · FEBRUARY 2014

Impact Factor: 2.59 · DOI: 10.1021/ie402739s

CITATIONS

3

READS

27

7 AUTHORS, INCLUDING:



Yue Yuan

Sichuan University

8 PUBLICATIONS 8 CITATIONS

SEE PROFILE



Bo Lai

Sichuan University

25 PUBLICATIONS 196 CITATIONS

SEE PROFILE



Ping Yang

45 PUBLICATIONS 842 CITATIONS

SEE PROFILE

Removal of High-Concentration C.I. Acid Orange 7 from Aqueous Solution by Zerovalent Iron/Copper (Fe/Cu) Bimetallic Particles

Yue Yuan,[†] Huiqiang Li,[†] Bo Lai,^{*,†} Ping Yang,[†] Min Gou,[†] Yuexi Zhou,[‡] and Guozhen Sun[§]

[†]Department of Environmental Science and Engineering, School of Architecture and Environment, Sichuan University, Chengdu 610065, China

[‡]Research Center of Water Pollution Control Technology, Chinese Research Academy of Environmental Sciences, Beijing 100012, China

[§]Beijing Energy & Environmental Protection Technology Co., Ltd., Beijing 100600, China

ABSTRACT: The removal of high-concentration C.I. acid orange 7 (AO7) in aqueous solution by the prepared iron/copper (Fe/Cu) bimetallic particles and zerovalent iron (ZVI) was investigated thoroughly. Fe/Cu bimetallic particles were prepared by planting Cu on the surface of Fe. Experimental results confirmed the superiority of Fe/Cu bimetallic particles for the degradation of AO7 in aqueous solution. Under the optimal conditions ($[\text{Fe/Cu}]_0 = 40 \text{ g}\cdot\text{L}^{-1}$, $[\text{AO7}]_0 = 1000 \text{ mmol}\cdot\text{L}^{-1}$, initial pH = 6.5, $\text{TML}_{\text{Cu}} = 0.62 \text{ g of Cu/g of Fe}$), the AO7 concentration and chemical oxygen demand (COD) and total organic carbon (TOC) removal efficiencies could reach 94.3%, 61.8%, and 60.8%, respectively, after only 10 min of treatment by Fe/Cu bimetallic particles. Under the same conditions, however, the AO7 concentration and COD and TOC removal efficiencies by ZVI only reached 35.5%, 25.1%, and 21.2%, respectively. Thus, the planting of Cu could improve the reactivity of Fe. The degradation of AO7 was analyzed by UV–vis and Fourier transform infrared spectra, and the results show that the chromophore part (i.e., $-\text{N}=\text{N}-$) of AO7 could be destructed by Fe/Cu bimetallic particles. Additionally, its degradation products might be sulfanilamide and 1-amino-2-naphtol, which would be removed by further mineralization of Fe/Cu bimetallic particles or sedimentation of Fe ions. Therefore, the Fe/Cu bimetallic system is a promising process for the toxic and refractory wastewater from the printing and dyeing industry.

1. INTRODUCTION

Because wastewater from the printing and dyeing industry can be highly colored and difficult to decompose, the negative effect of dyeing wastewater on the receiving water has brought about wide attention. Dyeing wastewater usually contained some toxic and refractory pollutants, so it could not be treated directly by a traditional biological treatment system. The physicochemical treatment processes, such as physical adsorption,¹ electro-Fenton,² and Fenton and Fenton-like reactions,^{3,4} are usually applied to treat dyeing wastewater to decompose its refractory pollutants and improve its biodegradability. However, all of these physicochemical processes suffer from the limitations of high equipment or running costs.

According to the study of previous authors, it is clear that Fe^0 /granular activated carbon (GAC) or zerovalent iron (ZVI) is a cost-effective method for the degradation of toxic and refractory pollutants, but they both suffer from the problem of filler passivation after long-term operation.⁵ Additionally, only under acidic conditions (pH < 5.0) could high decolorizing efficiencies of azo dyes in dyeing wastewater be obtained by ZVI.^{6,7} However, ZVI will be quickly consumed under acidic conditions, which will reduce the operational life span of ZVI seriously. Ultrasonic irradiation could enhance the reduction reactivity of Fe^0 /GAC or ZVI remarkably.^{7,8} However, ultrasonic irradiation would suffer from the limitations of high energy consumption and equipment costs. Therefore, affordable processes using low-cost materials and matching or exceeding the capability of conventional treatment processes are needed.

Not only could ultrasonic irradiation promote the reactivity of ZVI, but also the metal copper (Cu) could improve its reactivity because of the high standard reduction potential difference (0.78 V) between Cu and Fe^0 .^{9–11} Meanwhile, platinum (Pt) was also used to improve the reactivity of ZVI,^{12,13} but it suffers from the limitations of high costs. The previous authors found that Cu planted on the surface of iron particles (Fe^0) by a Fe and Cu replacement reaction could enhance the reactivity of Fe^0 remarkably, and the prepared Fe/Cu bimetallic particles were mainly used for dechlorination of a low-concentration organohalide ($<200 \mu\text{mol}\cdot\text{L}^{-1}$).^{14–17} In the literature, however, there is no report on the degradation of high-concentration dyeing wastewater ($>1000 \text{ mg}\cdot\text{L}^{-1}$) by Fe/Cu bimetallic particles.

In order to study the reactivity of Fe/Cu bimetallic particles for high-concentration dyeing wastewater, AO7 was used as a model pollutant to be degraded by the prepared Fe/Cu bimetallic particles in this study. The effect of the operating parameters on the AO7 removal efficiency by Fe/Cu bimetallic particles was investigated thoroughly. Meanwhile, under the optimal operating conditions of a Fe/Cu bimetallic system, the mineralization process of AO7 was further investigated by chemical oxygen demand (COD), total organic carbon (TOC),

Received: August 21, 2013

Revised: January 20, 2014

Accepted: January 22, 2014

Published: January 22, 2014

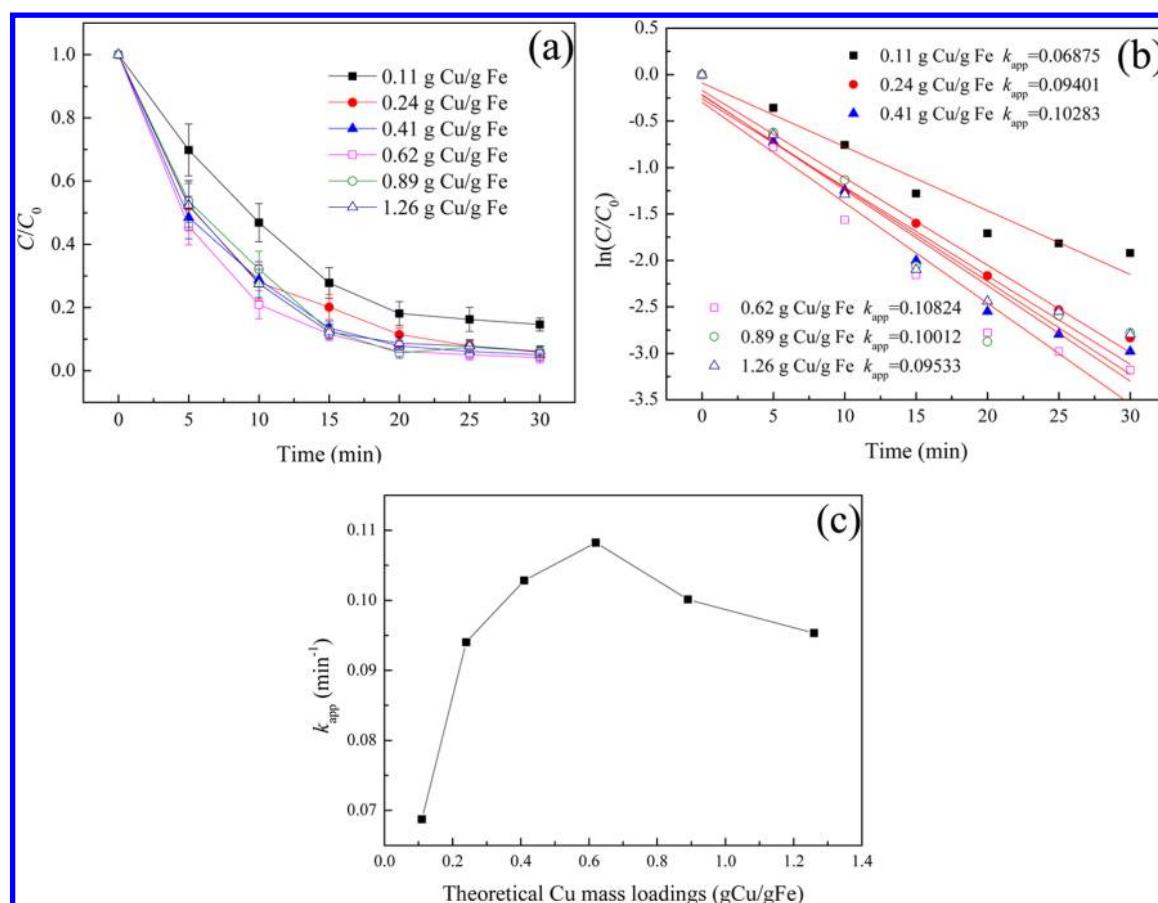


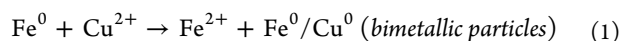
Figure 1. Degradation kinetics for AO7 by Fe/Cu bimetallic particles with different TML_{Cu} values. Experimental conditions: [AO7]₀ = 1000 mg·L⁻¹, initial pH = 6.5, [Na₂SO₄]₀ = 50 mmol·L⁻¹, [Fe/Cu]₀ = 15 g·L⁻¹, and stirring speed = 400 rpm.

and UV–vis and Fourier transform infrared (FTIR) spectrometry.

2. EXPERIMENTAL SECTION

2.1. Reagents. AO7 (98%), Na₂SO₄ (analytical reagent), CuSO₄·5H₂O (analytical reagent), and zerovalent iron (ZVI) powders purchased from Chengdu Kelong chemical reagent factory were used in the experiment. The ZVI powders have a mean particle size of approximately 120 μm, and their Fe content reaches approximately 97%. Deionized water was used in all experiments.

2.2. Bimetallic Particle Preparation. On the basis of the high standard reduction potential difference (0.78 V) between Cu and Fe, Cu was deposited on the surface of Fe⁰ by a simple metal displacement reaction in aqueous solution (eq 1).



On the basis of the prepared method of Fe/Cu bimetallic particles developed by the previous authors,^{18,19} these bimetallic particles used in this study were prepared via adding Fe⁰ to a CuSO₄ solution. Fe/Cu bimetallic particles with high theoretical Cu mass loadings (specifically, TML_{Cu} = 0.05, 0.11, 0.24, 0.41, 0.62, 0.89, and 1.26 g of Cu/g of Fe) were prepared to treat the high concentration the AO7 aqueous solution in this study.

2.3. Batch Experiments. The removal of the AO7 aqueous solution by Fe/Cu bimetallic particles was investigated thoroughly in batch experiments. AO7 aqueous solutions with different concentrations (1000–10000 mg·L⁻¹) were prepared

by simple dissolution in deionized water; meanwhile, Na₂SO₄ as an electrolyte (50 mmol·L⁻¹) was added into the AO7 aqueous solution. The prepared AO7 aqueous solutions were stocked in amber bottles. Additionally, AO7 stock solutions were not buffered. In each batch experiment, 200 mL of the AO7 aqueous solution and the desired Fe/Cu bimetallic particles were added in a 500 mL beaker, and the slurry was stirred by a mechanical stirrer with a stirring speed of 400 rpm. The whole experimental process was realized at 26 ± 3 °C. In this study, the key effect factors including theoretical Cu mass loadings (TML_{Cu} = 0–1.26 g of Cu/g of Fe), initial concentration of Fe/Cu bimetallic particles (5–50 g·L⁻¹), initial AO7 concentration (1000–10000 mg·L⁻¹), initial pH (3.0–8.0), and stirring speed (0–400 rpm) were investigated thoroughly in the batch experiments. Samples (1 mL) were taken at 5 min intervals during a 30 min treatment process, diluted by deionized water, and filtered through a poly(tetrafluoroethylene) syringe filter disk (0.45 μm). The diluted and filtered samples were analyzed by COD and TOC analyzers, respectively. Also, the residual AO7 concentration in the effluent was obtained by measuring the absorbance of the samples at 483 nm. Furthermore, under optimal conditions, the effluents of the batch experiments were analyzed by a UV–vis spectrophotometer (Shimazu, Japan) and a FTIR spectrometer (Perkin-Elmer 100).

2.4. Analytical Methods. The surface morphology and elementary composition of the prepared Fe/Cu bimetallic particle were observed by scanning electron microscopy (SEM) and energy-dispersive spectrometry (EDS; S-3500N, Hitachi,

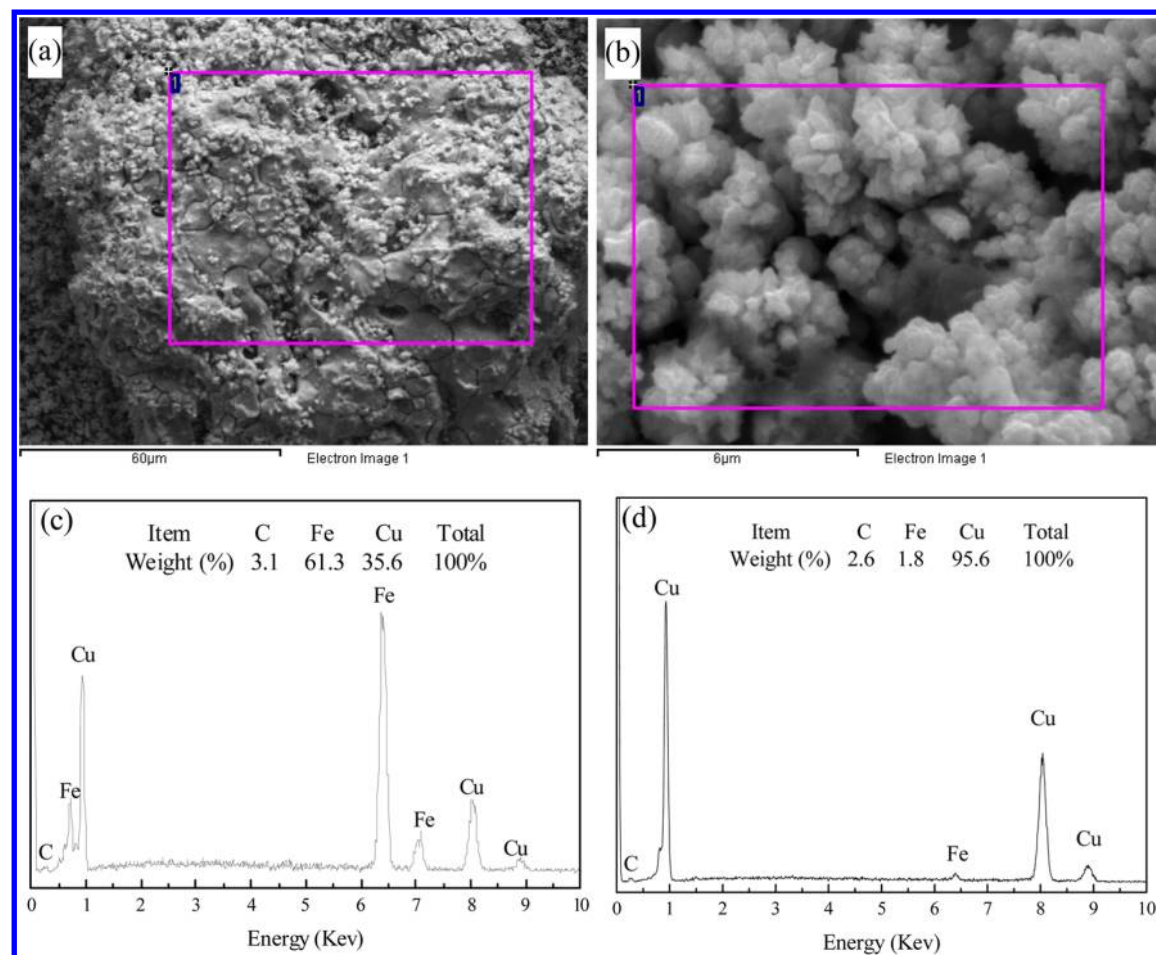


Figure 2. SEM and EDS spectra of the Fe/Cu bimetallic particle with an optimal TML_{Cu} of 0.62 g of Cu/g of Fe: (a) SEM image of the Fe/Cu bimetallic particle. (b) SEM image of planted Cu. (c) EDS spectrum of the area in the purple frame of the SEM in part a. (d) EDS spectrum of the area in the purple frame of the SEM in part b.

Japan).^{5,20} FTIR was used to assess the differences in the general functional groups of the samples, and the FTIR analysis method was shown in our previous work.²¹ Each sample was scanned four times between the wavelengths of 4000 and 400 cm^{-1} . The UV–vis absorption spectra of the samples were carried out in 10 mm quartz cuvettes, and the UV–vis spectra were recorded from 190 to 650 nm. The concentration of AO7 was measured by determining its absorbance at λ_{max} (483 nm) in a cuvette with a 1 cm cell length and calculating its weight/volume concentration based on a standard curve.²² TOC and COD of the samples were measured by TOC (Shimadzu, Japan) and COD (Lianhua, China) analyzers, respectively.

3. RESULTS AND DISCUSSION

3.1. Effect of the Theoretical Cu Mass Loading (TML_{Cu}). In order to investigate the effect of TML_{Cu} on the removal of the high-concentration AO7 in an aqueous solution by a Fe/Cu bimetallic system, the batch experiments using the prepared Fe/Cu bimetallic particles with different TML_{Cu} were set up to treat the AO7 aqueous solution (1000 $mg \cdot L^{-1}$). Batch experiments were carried out by adding 3.0 g of different weight ratios of Fe/Cu bimetallic particles into a beaker ($[Fe/Cu]_0 = 15 \text{ g} \cdot L^{-1}$), in which each beaker included 200 mL of the AO7 aqueous solution with an initial concentration of 1000 $mg \cdot L^{-1}$, an initial pH at 6.5, and a Na_2SO_4 concentration of 50 $mmol \cdot L^{-1}$. The AO7 aqueous solution and Fe/Cu bimetallic particles

were mixed completely by a mechanical agitator with a stirring speed of 400 rpm. Finally, the AO7 residual concentration at the desired treatment time was determined by a UV–vis spectrophotometer.

Figure 1a shows the effect of different TML_{Cu} values on the removal of AO7 in an aqueous solution by Fe/Cu bimetallic particles, and the experimental data were used to compute the apparent rate constants (k_{app}) for the removal of AO7 by Fe/Cu bimetallic particles. The logarithmic plots of the AO7 residual concentration in an aqueous solution versus the treatment time are shown in Figure 1b, which illustrate that a good linear fitting was observed in each of the batch experiments, and their correlation coefficient (R^2) all were above 0.87. The results reveal that the AO7 removal efficiencies by Fe/Cu bimetallic particles could be described by the pseudo-first-order reaction. Furthermore, it can be observed from Figure 1c that k_{app} for the degradation of AO7 increased remarkably from 0.06875 to 0.10824 min^{-1} with an increase of TML_{Cu} from 0.11 to 0.62 g of Cu/g of Fe, and then k_{app} began to decrease gradually with a continuous increase of TML_{Cu} .

Cu planting on the surface of Fe^0 could result in the formation of a galvanic couple between Cu (cathode) and Fe^0 (anode), and the potential difference (0.777 V) between Cu and Fe was much higher than that (0.440 V) between C and $Fe^{9,11,21}$. According to eqs 2–4, therefore, it is clear that planting Cu could promote the corrosion rate of Fe^0 , which

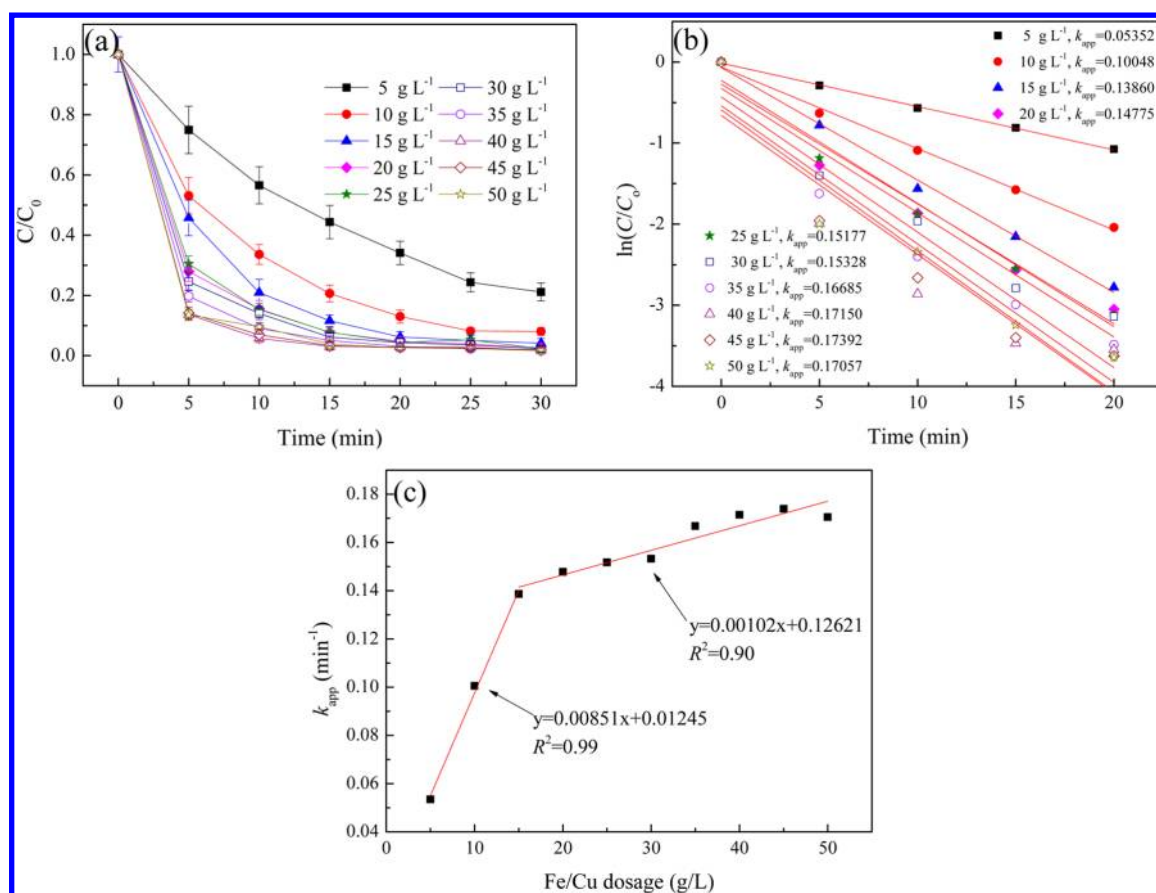
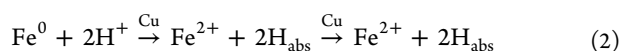


Figure 3. Degradation kinetics for AO7 by the Fe/Cu bimetallic particle with different additions of Fe/Cu bimetallic particles. Experimental conditions: $[AO7]_0 = 1000 \text{ mg}\cdot\text{L}^{-1}$, initial pH = 6.5, $[Na_2SO_4]_0 = 50 \text{ mmol}\cdot\text{L}^{-1}$, $TML_{Cu} = 0.62 \text{ g of Cu/g of Fe}$, and stirring speed = 400 rpm.

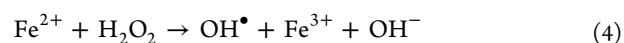
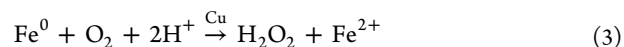
could facilitate the generation of absorbed hydrogen (H_{abs}) or hydroxyl radical (OH^\bullet) under anoxic or oxic conditions.^{18,23,24}

In other words, planting Cu served as a catalyst during the corrosion reaction process of Fe^0 , and it could accelerate the release of electrons from Fe^0 and generate H_{abs} or OH^\bullet . Meanwhile, other transition metals such as palladium (Pd) also could play a similar role on the corrosion of Fe^0 and improve its reactivity.^{25,26} In this study, the degradation of AO7 mainly resulted from the redox of the generated H_{abs} or OH^\bullet . Therefore, the increase of TML_{Cu} could increase remarkably the formation number of the galvanic couples between Cu (cathode) and Fe^0 (anode) when TML_{Cu} was lower than 0.62 g of Cu/g of Fe. Subsequently, the continuous increase of TML_{Cu} could decrease the formation number of the galvanic couples because of the gradual decrease of the proportion of Fe^0 in bimetallic particles. Furthermore, excess Cu was difficult to deposit on the surface of Fe^0 and easy to drop off to form fine Cu particles. The shedding fine Cu particles did not easily contact with Fe^0 , which could affect the formation of the galvanic couples between Cu (cathode) and Fe^0 (anode). The previous authors also found similar results, but its TML_{Cu} was very low ($<30 \mu\text{mol of Cu/g of Fe}$).¹⁷ According to the above experimental results, it is clear that the optimal TML_{Cu} for treatment of the AO7 aqueous solution was 0.62 g of Cu/g of Fe.

Under anoxic conditions



Under oxic conditions



3.2. Characterizing Fe/Cu Bimetallic Particles. In order to observe the distribution of planting Cu on the surface of Fe^0 , several important properties of the Fe/Cu bimetallic particle with an optimal TML_{Cu} (0.62 g of Cu/g of Fe), including the surface morphology and elementary composition, were analyzed by SEM and EDS, respectively.

The dispersion of Cu on the surface of Fe^0 significantly affects the reactivity of the prepared Fe/Cu bimetallic particles.²⁷ In this study, it can be seen from Figure 2a that the morphology of the prepared Fe/Cu bimetallic particles with an optimal TML_{Cu} (0.62 g of Cu/g of Fe) was observed by SEM. Simultaneously, the surface elementary composition was obtained by EDS to analyze the area in the purple frame of the SEM image (Figure 2a). Meanwhile, the results of EDS analysis are shown in Figure 2c. It can be seen from Figure 2a that there were many fine particles on the surface of the Fe^0 particle, and a large number of the fine particles also were found in the surrounding area of the Fe/Cu bimetallic particles. Furthermore, the characteristics of these fine particles were analyzed by SEM and EDS with a higher magnification (Figure 2b). It is clear that these fine particles had an irregular shape and their main elemental constituent was Cu (94.2 wt %). The results suggest that these fine particles were the planted Cu particles, and only part of these fine Cu particles could affix to the surface

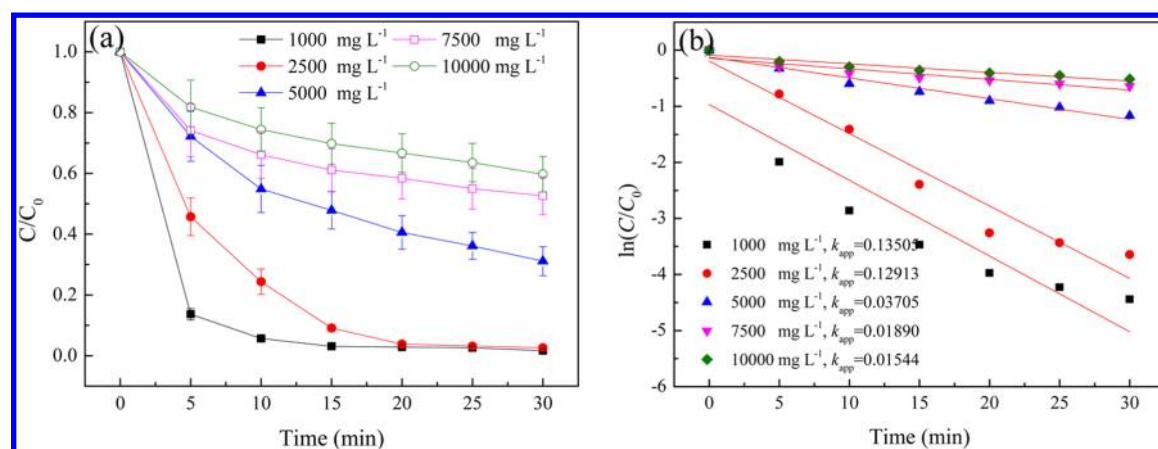


Figure 4. Degradation kinetics for AO7 by Fe/Cu bimetallic particles with different initial concentrations of AO7. Experimental conditions: $[\text{Fe}/\text{Cu}]_0 = 40 \text{ g}\cdot\text{L}^{-1}$, initial pH = 6.5, $[\text{Na}_2\text{SO}_4]_0 = 50 \text{ mmol}\cdot\text{L}^{-1}$, $\text{TML}_{\text{Cu}} = 0.62 \text{ g}$ of Cu/g of Fe, and stirring speed = 400 rpm.

of the Fe^0 particle and the residual fine Cu particles all dropped off. Stephen et al. found that the Cu mass loading on the surface of the Fe^0 particle would almost not increase when it reached $30 \mu\text{mol}$ of Cu/g of Fe (i.e., 0.00192 g of Cu/g of Fe).¹⁷ In this study, however, the optimal TML_{Cu} (0.62 g of Cu/g of Fe) was much higher than the actual Cu mass loading (approximate 0.00192 g of Cu/g of Fe) on the surface of Fe^0 particles. The results could be explained as not only did the fine Cu particles affix to the surface of Fe^0 particles but also the deciduous fine Cu particles could form galvanic couples with Fe^0 (anode). Especially under the stirring conditions, the fluidizing fine Cu particles and Fe/Cu bimetallic particles would collide with each other, and the intercollision between the Cu and Fe/Cu bimetallic particles could form galvanic couples, which could improve the reactivity of the prepared Fe/Cu bimetallic particles. Therefore, despite the dropoff of excess TML_{Cu} , they also could enhance the degradation capacity of Fe/Cu bimetallic particles for AO7 in an aqueous solution.

3.3. Effect of Fe/Cu Bimetallic Particle Addition on the Removal of AO7. On the basis of Figure 3a, AO7 removal varied with a dosage of Fe/Cu bimetallic particles (5, 10, 15, 20, 25, 30, 35, 40, 45, and $50 \text{ g}\cdot\text{L}^{-1}$). Their TML_{Cu} values all were 0.62 g of Cu/g of Fe. The removal efficiencies of AO7 increased from 78.85% to 98.19% after 30 min of reaction when the amount of Fe/Cu bimetallic particles increased from 5 to $40 \text{ g}\cdot\text{L}^{-1}$ (Figure 3a). The removal of AO7 in an aqueous solution with different amounts of Fe/Cu bimetallic particles all followed pseudo-first-order kinetics, and their correlation coefficients (R^2) were all above 0.85 (Figure 3b). In light of previously reported experimental results, the removal efficiencies or apparent rate constant (k_{app}) of the pollutants all could increase with an increase in the addition of metal catalyst or reductant.^{28,29} From Figure 3b, k_{app} for the degradation of AO7 increased rapidly from 0.05352 to 0.13860 min^{-1} when the amount of Fe/Cu bimetallic particles increased from 5 to $15 \text{ g}\cdot\text{L}^{-1}$, and then k_{app} continued to increase gradually and exceed 0.17 min^{-1} when the amount of Fe/Cu bimetallic particles was above $40 \text{ g}\cdot\text{L}^{-1}$.

As shown in Figure 3c, the data were plotted as k_{app} versus the amount of Fe/Cu bimetallic particles ($[\text{Fe}/\text{Cu}]_0$). At the initial phase ($5 \text{ g}\cdot\text{L}^{-1} < [\text{Fe}/\text{Cu}]_0 < 15 \text{ g}\cdot\text{L}^{-1}$), k_{app} and $[\text{Fe}/\text{Cu}]_0$ had a good linear relationship and the correlation coefficient (R^2) reached 0.99, which indicated that k_{app} was proportional to the amount of Fe/Cu bimetallic particles and

k_{app} could be improved by elevating the initial concentration of Fe/Cu bimetallic particles. At the second phase ($15 \text{ g}\cdot\text{L}^{-1} < [\text{Fe}/\text{Cu}]_0 < 50 \text{ g}\cdot\text{L}^{-1}$), k_{app} and $[\text{Fe}/\text{Cu}]_0$ also had a good linear relationship and the correlation coefficient (R^2) reached 0.90. However, k_{obs} (0.00851 min^{-1}) at the initial phase was 8 times higher than that (0.00102 min^{-1}) at the second phase.

As a result, the removal efficiency or first-order rate constant for AO7 could increase with an increase in the amount of Fe/Cu bimetallic particles. Because degradation of AO7 was mainly carried out by the reactive sites on the surface of Fe/Cu bimetallic particles, an increase in the amount of Fe/Cu bimetallic particles could simultaneously increase the number of active sites, resulting in an improvement of the degradation of AO7. Similar results also were obtained in the ZVI system; the degradation efficiency increased with an increase of the Fe^0 dosage.³⁰ Furthermore, the slow increase of k_{app} for AO7 degradation at the second phase ($15 \text{ g}\cdot\text{L}^{-1} < [\text{Fe}/\text{Cu}]_0 < 50 \text{ g}\cdot\text{L}^{-1}$) could be explained by the fact that the key limiting factor had been changed from the amount of Fe/Cu bimetallic particles to the mass-transfer rate of AO7 and its intermediates between the solution phase and the surface of Fe/Cu bimetallic particles. The degradation efficiency of the pollutants in wastewater usually was inhibited by the lower mass-transfer rate of the pollutants, intermediates, and products.^{31–33} Despite the fact that $15 \text{ g}\cdot\text{L}^{-1}$ Fe/Cu addition is high enough to provide sufficient reactive capacity, $40 \text{ g}\cdot\text{L}^{-1}$ Fe/Cu addition was chosen as the optimal metal addition in the following experiments to obtain a higher removal efficiency (>98%).

3.4. Effect of the Initial Concentration of AO7. Five different initial concentrations of the AO7 aqueous solution (1000, 2500, 5000, 7500, and $10000 \text{ mg}\cdot\text{L}^{-1}$) were investigated at fixed Fe/Cu addition ($40 \text{ g}\cdot\text{L}^{-1}$) and TML_{Cu} (0.62 g of Cu/g of Fe). From the data (Figure 4a), AO7 is almost completely degraded within 20 min only when the initial AO7 concentration was below $2500 \text{ mg}\cdot\text{L}^{-1}$. The degradation of AO7 with different initial concentrations (1000 – $10000 \text{ mg}\cdot\text{L}^{-1}$) all followed a pseudo-first-order kinetics, and their correlation coefficients (R^2) were all above 0.85 (Figure 4b). However, k_{app} of AO7 degradation decreased sharply from 0.13505 to 0.01544 min^{-1} when the initial concentration of AO7 increased from 1000 to $10000 \text{ mg}\cdot\text{L}^{-1}$. The results suggest that the removal efficiency of Fe/Cu bimetallic particles would be limited by a higher initial concentration of AO7. The degradation of AO7 in a Fe/Cu bimetallic particle system is a

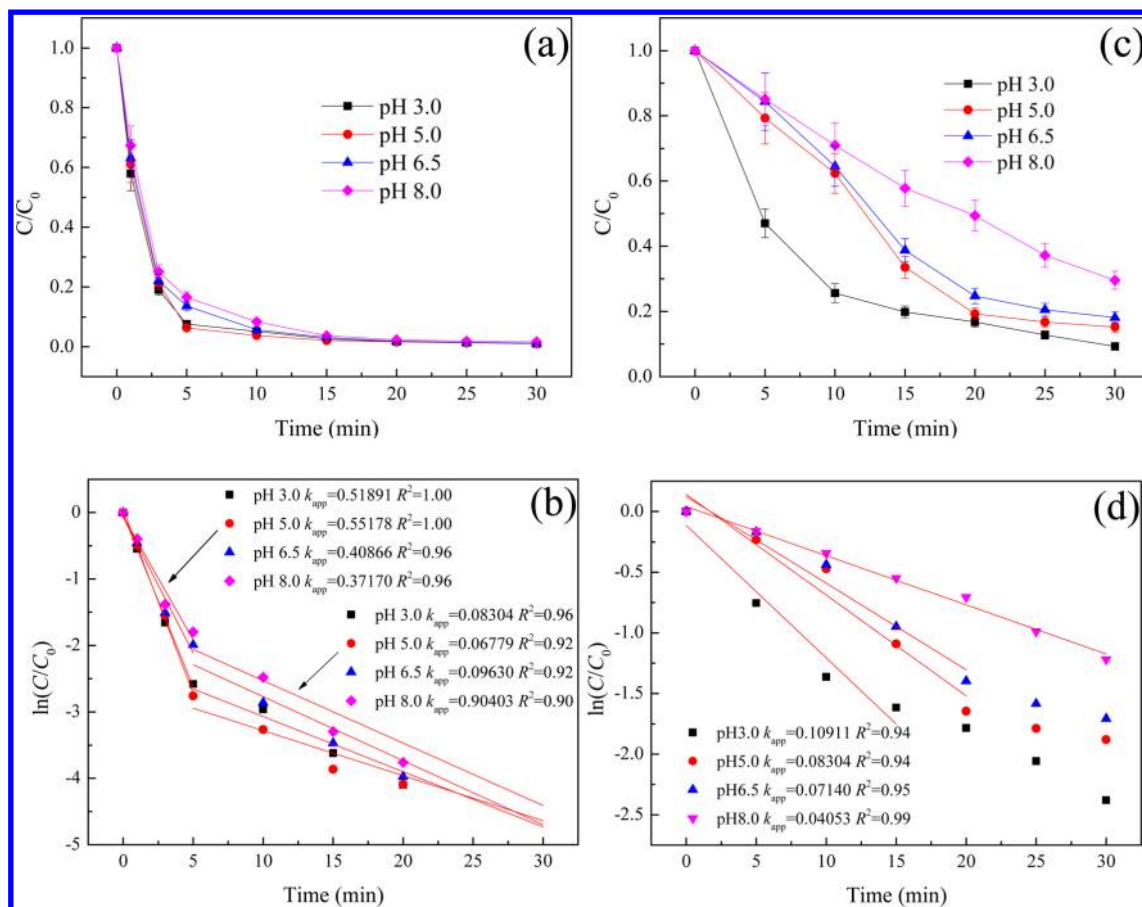


Figure 5. Degradation kinetics for AO7 by Fe/Cu bimetallic particles or ZVI with different initial pH values: (a and b) Fe/Cu bimetallic experiments; (c and d) ZVI control experiments. Experimental conditions: $[\text{Fe/Cu}]_0 = 40 \text{ g}\cdot\text{L}^{-1}$, $[\text{Fe}^0]_0 = 40 \text{ g}\cdot\text{L}^{-1}$, $[\text{AO7}]_0 = 1000 \text{ mmol}\cdot\text{L}^{-1}$, $[\text{Na}_2\text{SO}_4]_0 = 50 \text{ mmol}\cdot\text{L}^{-1}$, $\text{TML}_{\text{Cu}} = 0.62 \text{ g}$ of Cu/g of Fe, and stirring speed = 400 rpm.

heterogeneous reaction, which involves adsorption of AO7 on the reactive sites of Fe/Cu bimetallic particles, degradation reaction, and release of the degradation products. A higher initial concentration ($>2500 \text{ mg}\cdot\text{L}^{-1}$) of AO7 would lead to competitive adsorption among AO7 molecules because the adsorption reaction area of Fe/Cu is fixed. Meanwhile, a higher initial concentration of AO7 would generate a higher concentration of intermediates, and the intermediates also would compete with AO7. In other words, the mass-transfer rate of AO7 and intermediates between the solution phase and the surface of Fe/Cu bimetallic particles would become mainly a limiting factor when the initial concentration of AO7 was above $2500 \text{ mg}\cdot\text{L}^{-1}$. Additionally, Fang et al. had found similar results when they used Ni/Fe bimetallic particles to degrade decabromodiphenyl ether (BDE209).²⁹ In the literature, the treatment efficiency of ZVI usually was limited by the mass-transfer efficiency of pollutants, intermediates, and corrosion products.^{31–33}

3.5. Effect of the Initial pH of the AO7 Aqueous Solution. The initial pH of the reaction system is known to affect the decolorizing efficiency of azo dyes by a ZVI system. Only under acidic conditions ($\text{pH} < 5.0$) could a high decolorizing efficiency be obtained by ZVI.^{6,7} However, ZVI will be quickly corroded and consumed under acidic conditions, which will seriously reduce the operational life span of ZVI. Therefore, the removal of AO7 by a ZVI system under neutral conditions became most significant. To thoroughly evaluate the effect of the initial pH on the removal of AO7 in the aqueous

solution, a Fe/Cu bimetallic system and a ZVI system with different initial pH values (3.0, 5.0, 6.5, and 8.0) were set up, and the rest of the operating conditions for the two experimental systems were the same (i.e., $[\text{Fe/Cu}]_0 = [\text{Fe}^0]_0 = 40 \text{ g}\cdot\text{L}^{-1}$, $[\text{AO7}]_0 = 1000 \text{ mmol}\cdot\text{L}^{-1}$, $[\text{Na}_2\text{SO}_4]_0 = 50 \text{ mmol}\cdot\text{L}^{-1}$, and stirring speed = 400 rpm). Figure 5a shows that all of the AO7 removal efficiencies were above 98% after 30 min of treatment by Fe/Cu bimetallic particles under the conditions of different initial pH values of 3.0, 5.0, 6.5, and 8.0. However, lower AO7 removal efficiencies (70–90%) in the ZVI system were obtained after 30 min of treatment, and their removal efficiencies dropped rapidly from 90% to 70% with an increase of the initial pH value from 3.0 to 8.0 (Figure 5c).

It can be seen from Figure 5b that degradation of AO7 by Fe/Cu bimetallic systems with different initial pH values (3.0–8.0) all followed pseudo-first-order kinetics. At the initial stage (0–5 min), their correlation coefficients (R^2) were all above 0.96, and their k_{app} values decreased from 0.51891 to 0.37170 min^{-1} gradually with an increase of the initial pH from 3.0 to 8.0 (Figure 5b). The results suggest that the degradation capacity of a Fe/Cu bimetallic system also would be affected slightly by the initial pH. At the second stage (5–30 min), however, their k_{app} values remain between 0.06779 and 0.09630 min^{-1} , which were much lower than those at the initial stage (0–5 min). This phenomenon could be explained by the fact that a large part ($>80\%$) of AO7 in an aqueous solution could be rapidly removed by a Fe/Cu bimetallic system after only 5 min of treatment and the residual AO7 would be removed

gradually in the second stage (5–30 min). In other words, the removal rate of AO7 at the initial stage (0–5 min) was much higher than that at the second stage (5–30 min). From Figure 5b,d, it is clear that k_{app} of the ZVI system decreased sharply from 0.10911 to 0.04053 min^{-1} when the initial pH increased from 3.0 to 8.0, and their k_{app} values were much lower than those of a Fe/Cu bimetallic system. In particular, k_{app} (0.37170 min^{-1}) of a Fe/Cu bimetallic system was 9 times higher than that (0.04053 min^{-1}) of a ZVI system when the initial pH was 8.0.

The results reveal that the AO7 removal efficiency of Fe/Cu bimetallic particles was slightly influenced by the initial pH, while that of the ZVI system was seriously affected by the initial pH. The previous authors have also found that only under the acidic condition ($\text{pH} < 5$) could a high pollutant removal efficiency be achieved by the ZVI system.^{21,31,34} In a Fe/Cu bimetallic system, the planted copper (Cu) could improve the reactivity of ZVI because of the high standard reduction potential difference (0.78 V) between Cu and Fe.⁹ Furthermore, the galvanic couple formed between Cu (cathode) and Fe^0 (anode) could promote the corrosion rate of Fe^0 , which could facilitate the generation of absorbed hydrogen (H_{abs}) or hydroxyl radical (OH^\bullet) under anoxic or oxic conditions.^{18,23,24} Thus, AO7 in an aqueous solution also could be degraded effectively by the generated H_{abs} or OH^\bullet even if the initial pH was 8.0.

3.6. Mineralization of AO7 in an Aqueous Solution. In order to investigate the mineralization of AO7, the COD and TOC of the treatment effluent of a Fe/Cu bimetallic system and a ZVI control system (under optimal conditions) were determined at 5 min intervals in the whole 30 min treatment process. From Figure 6, it is clear that the curves of Fe/Cu

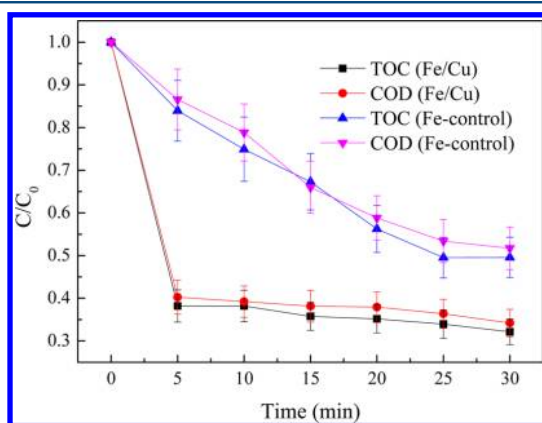


Figure 6. Variation of COD and TOC of an AO7 aqueous solution during the treatment process by Fe/Cu bimetallic particles or ZVI. Experimental conditions: $[\text{AO7}]_0 = 1000 \text{ mmol}\cdot\text{L}^{-1}$, $\text{COD}_0 = 1218 \text{ mg}\cdot\text{L}^{-1}$, $\text{TOC}_0 = 303 \text{ mg}\cdot\text{L}^{-1}$, $[\text{Fe/Cu}]_0 = 40 \text{ g}\cdot\text{L}^{-1}$, initial $\text{pH} = 6.5$, $[\text{Na}_2\text{SO}_4]_0 = 50 \text{ mmol}\cdot\text{L}^{-1}$, $\text{TML}_{\text{Cu}} = 0.62 \text{ g of Cu/g of Fe}$, and stirring speed = 400 rpm.

bimetallic particles illustrate that COD and TOC removal efficiencies increased rapidly to 61.8% and 59.8% after only 5 min of treatment, respectively, and then the values continued to increase gradually to 67.9% and 65.8% in the subsequent 25 min treatment process. The varying trend of COD and TOC removal efficiencies was very similar to that of the AO7 removal efficiency in the whole 30 min treatment process (Figure 5a). The results indicate that a Fe/Cu bimetallic system could decompose AO7 into small molecular compounds in the initial

5 min, but these compounds could hardly be further mineralized into CO_2 and H_2O in the subsequent treatment process. The high TOC and COD removal efficiencies might also have resulted from coprecipitation and enmeshment of the ferrous and ferric hydroxide floc for the degradation products of AO7 (i.e., small molecular compounds).

In the whole 30 min treatment process, however, the COD and TOC removal efficiencies by a ZVI control experiment increased gradually to 51.4% and 48.2%, respectively (Figure 6). Their varying trend was also similar to the trend of the AO7 removal efficiency in the whole 30 min treatment process by a ZVI system (Figure 5c). The results also suggest that AO7 only could be decomposed into small molecular compounds after 30 min of treatment by a ZVI system.

However, the mineralization efficiency of a Fe/Cu bimetallic system was much higher than that of a ZVI control system. Specifically, after 5 min of treatment, the TOC and COD removal efficiencies (i.e., 61.8% and 59.8%) of a Fe/Cu bimetallic system were 3 times higher than those (i.e., 19.1% and 13.4%) of a ZVI control system. Thus, the planting of Cu could improve the reactivity of ZVI.

3.7. UV–Vis and FTIR Spectral Analysis. Figure 7 shows typical UV–vis spectra obtained during the degradation of AO7

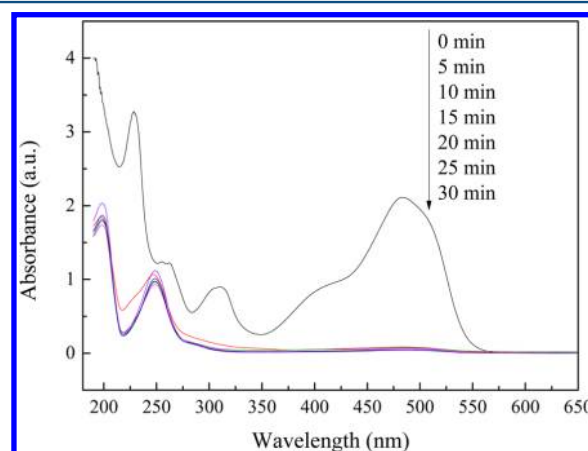


Figure 7. Variation of UV–vis spectra of an AO7 aqueous solution during the treatment process by using Fe/Cu bimetallic particles. Experimental conditions: $[\text{Fe/Cu}]_0 = 40 \text{ g}\cdot\text{L}^{-1}$, $[\text{AO7}]_0 = 1000 \text{ mmol}\cdot\text{L}^{-1}$, initial $\text{pH} = 6.5$, $[\text{Na}_2\text{SO}_4]_0 = 50 \text{ mmol}\cdot\text{L}^{-1}$, $\text{TML}_{\text{Cu}} = 0.62 \text{ g of Cu/g of Fe}$, and stirring speed = 400 rpm.

in an aqueous solution by Fe/Cu bimetallic particles under optimal conditions. The spectrum obtained prior to the degradation process (0 min) is characterized by two peaks in the visible region, corresponding to the zao form (430 nm) and the hydrazone form (485 nm) of AO7.³⁵ These forms originate from intermolecular hydrogen-bonding tautomeric interactions between the β -hydrogen of the corresponding azo linkage and the oxygen of the naphthyl group, respectively.³⁵ The peaks in the UV region (310 and 228 nm) correspond to π – π^* transitions in the naphthalene and benzoic rings of AO7, respectively.³⁶ It can be seen from Figure 7 that all the four main peaks (228, 310, 430, and 485 nm) of AO7 were almost removed completely after only 5 min of treatment by Fe/Cu bimetallic particles. Meanwhile, two new peaks, located at 199 and 249 nm, were generated in the UV–vis spectrum (Figure 7). Liu et al. also found the similar new peaks after the degradation of AO7 by a Fe^0/GAC system in the presence of ultrasound.⁸ The results suggest that the zao form (430 nm)

and the hydrazone form (485 nm) of AO7 could be decomposed completely after 5 min of treatment by Fe/Cu bimetallic particles. However, complete removal of the peaks located 228 and 310 nm did not represent complete mineralization of the benzoic and naphthalene rings of AO7. The formation of the two new peaks (199 and 249 nm) might have resulted from the blue-shift effect of the benzoic and naphthalene rings when the azo group ($-\text{N}=\text{N}-$) of AO7 was broken by Fe/Cu bimetallic particles. The previous authors also reported that the similar new peaks might be associated with the generation of sulfanilamide and 1-amino-2-naphthol, which were the most probable products from metal Fe reduction of AO7.^{8,37}

The degradation of AO7 by Fe/Cu bimetallic particles was analyzed by FTIR spectroscopy, and the FTIR spectra of AO7 before and after degradation are shown in Figure 8. Trace a in

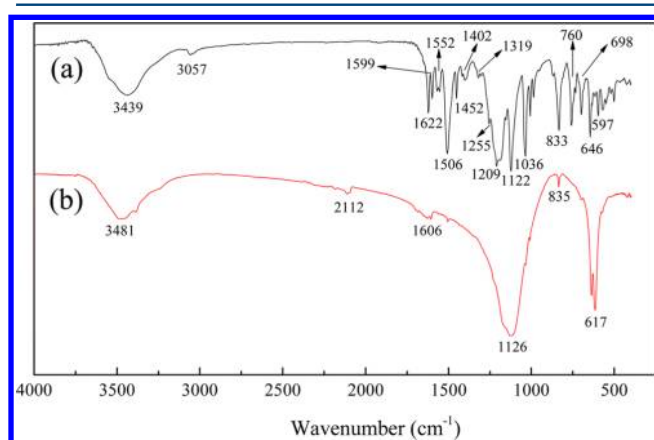


Figure 8. FTIR adsorption spectra of the 400–4000 cm^{-1} region of AO7 before and after treatment by a Fe/Cu bimetallic system: (a) AO7 without treatment; (b) AO7 after treatment. Experimental conditions: $[\text{Fe/Cu}]_0 = 40 \text{ g}\cdot\text{L}^{-1}$, $[\text{AO7}]_0 = 1000 \text{ mmol}\cdot\text{L}^{-1}$, initial pH = 6.5, $[\text{Na}_2\text{SO}_4]_0 = 50 \text{ mmol}\cdot\text{L}^{-1}$, $\text{TML}_{\text{Cu}} = 0.62 \text{ g of Cu/g of Fe}$, and stirring speed = 400 rpm.

Figure 8 represents the FTIR adsorption spectrum of AO7 without any degradation treatment. The peak at 1506 cm^{-1} is attributed to the bending vibration mode $\delta(\text{N}-\text{H})$ of the hydrazone form of AO7³⁸ or to the azo bond ($-\text{N}=\text{N}-$) vibrations³⁹ or aromatic ring vibrations sensitive to interaction with the azo bond.³⁵ The bands at 1452, 1553, 1599, and 1622 cm^{-1} are attributed to $\text{C}=\text{C}$ aromatic skeletal vibrations.⁴⁰ Additionally, the band at 1622 cm^{-1} is also assigned to a combination of phenyl ring vibrations with stretching of the $\text{C}=\text{N}$ group of the hydrazone form of the azo dye.⁴⁰ The bands located at 1319 and 1402 cm^{-1} can be linked to $\text{O}-\text{H}$ bending vibrations, while the band at 1255 cm^{-1} is linked to the stretching vibrations of $\text{C}-\text{N}$ of the hydrazone form of AO7.³⁹ Finally, the bands at 1036 and 1122 cm^{-1} are assigned to the coupling between benzene mode 1 and $\nu_s(\text{SO}_3)$, while the band at 1209 cm^{-1} is linked to the $\nu_{\text{as}}(\text{SO}_3)$ stretching mode.³⁸

Trace b in Figure 8 shows the FTIR adsorption spectrum of AO7 after 30 min of treatment by Fe/Cu bimetallic particles under optimal conditions. It is clear that the intensities of all peaks (1255 , 1506 , 1553 , and 1622 cm^{-1}) linked to the hydrazone form of AO7 decreased remarkably. In particular, the intensity decrease of the band at 1506 cm^{-1} reflects the destruction of the chromophore part (i.e., $-\text{N}=\text{N}-$) of AO7. Additionally, a broad and intense band between 850 and 1600

cm^{-1} occurred after treatment by Fe/Cu bimetallic particles, which resulted from the degradation products of AO7. Furthermore, the intensities of all peaks (1452 , 1553 , 1599 , and 1622 cm^{-1}) attributed to $\text{C}=\text{C}$ aromatic skeletal vibrations were also decreased sharply, which suggests that part of the degradation products (benzoic and naphthalene rings) of AO7 were removed by further mineralization of Fe/Cu bimetallic particles or sedimentation of Fe ions. The results also prove that the higher TOC and COD removal efficiencies obtained by Fe/Cu bimetallic particles were valid. Meanwhile, the results obtained by FTIR were according to UV–vis spectral analysis.

4. CONCLUSIONS

In this study, it was demonstrated that the prepared Fe/Cu bimetallic particles successfully remove AO7 from water and thus could be used for the treatment of printing and dyeing wastewater containing AO7. First, the effect of TML_{Cu} on the degradation of a high concentration of AO7 aqueous solution was investigated thoroughly, and the results suggest that the optimal TML_{Cu} was $0.62 \text{ g of Cu/g of Fe}$ for the degradation of AO7. The surface morphology and elementary composition of a Fe/Cu bimetallic particle with an optimal TML_{Cu} ($0.62 \text{ g of Cu/g of Fe}$) was analyzed by SEM and EDS, respectively. It was found that the heterogeneous Cu distribution on the surface of the Fe^0 particle could improve the reactivity of Fe/Cu bimetallic particles. Furthermore, under the same optimal conditions ($[\text{Fe/Cu}]_0 = 40 \text{ g}\cdot\text{L}^{-1}$, $[\text{AO7}]_0 = 1000 \text{ mmol}\cdot\text{L}^{-1}$, initial pH = 6.5, and $\text{TML}_{\text{Cu}} = 0.62 \text{ g of Cu/g of Fe}$), the AO7 degradation efficiency of Fe/Cu bimetallic particles was much higher than that of ZVI. In other words, the reactivity of Fe/Cu bimetallic particles was much stronger than that of ZVI. The analysis results of UV–vis and FTIR reveal that the azo bonds ($-\text{N}=\text{N}-$) of AO7 could be decomposed rapidly by Fe/Cu bimetallic particles, and its degradation products would be removed by further mineralization of Fe/Cu bimetallic particles or sedimentation of Fe ions. Therefore, the higher TOC and COD removal efficiencies (67.9% and 65.8%) obtained by Fe/Cu bimetallic particles were valid.

AUTHOR INFORMATION

Corresponding Author

*Tel./fax: +86 18682752302. E-mail: laibo1981@163.com.

Notes

The authors declare no competing financial interest.

ACKNOWLEDGMENTS

The authors acknowledge financial support from National Natural Science Foundation of China (Grant 21207094), a China postdoctoral science foundation special funded project (Grant 2013T60854), National Natural Science Foundation of China (Grant 31200068), and a special S&T project on the treatment and control of water pollution (Grant 2012ZX07201-005).

REFERENCES

- (1) Ahmad, A. A.; Hameed, B. H. Effect of preparation conditions of activated carbon from bamboo waste for real textile wastewater. *J. Hazard. Mater.* **2010**, *173* (1–3), 487–93.
- (2) Ruiz, E. J.; Arias, C.; Brillas, E.; Hernández-Ramírez, A.; Peralta-Hernández, J. M. Mineralization of Acid Yellow 36 azo dye by electro-Fenton and solar photoelectro-Fenton processes with a boron-doped diamond anode. *Chemosphere* **2011**, *82* (4), 495–501.

- (3) Kang, S. F.; Liao, C. H.; Po, S. T. Decolorization of textile wastewater by photo-fenton oxidation technology. *Chemosphere* **2000**, *41* (8), 1287–1294.
- (4) Kang, S. F.; Liao, C. H.; Chen, M. C. Pre-oxidation and coagulation of textile wastewater by the Fenton process. *Chemosphere* **2002**, *46* (6), 923–928.
- (5) Lai, B.; Zhou, Y. X.; Yang, P. Passivation of sponge iron and GAC in Fe⁰/GAC mixed-potential corrosion reactor. *Ind. Eng. Chem. Res.* **2012**, *51* (22), 7777–7785.
- (6) Deng, N.; Luo, F.; Wu, F.; Xiao, M.; Wu, X. Discoloration of aqueous reactive dye solutions in the UV/Fe⁰ system. *Water Res.* **2000**, *34* (8), 2408–2411.
- (7) Zhang, H.; Duan, L. J.; Zhang, Y.; Wu, F. The use of ultrasound to enhance the decolorization of the C.I. Acid Orange 7 by zero-valent iron. *Dyes Pigm.* **2005**, *65* (1), 39–43.
- (8) Liu, H.; Li, G.; Qu, J.; Liu, H. Degradation of azo dye Acid Orange 7 in water by Fe⁰/granular activated carbon system in the presence of ultrasound. *J. Hazard. Mater.* **2007**, *144* (1–2), 180–186.
- (9) Ma, L. M.; Ding, Z. G.; Gao, T. Y.; Zhou, R. F.; Xu, W. Y.; Liu, J. Discoloration of methylene blue and wastewater from a plant by a Fe/Cu bimetallic system. *Chemosphere* **2004**, *55* (9), 1207–12.
- (10) Ghauch, A.; Assi, H. A.; Bdeir, S. Aqueous removal of diclofenac by plated elemental iron: Bimetallic systems. *J. Hazard. Mater.* **2010**, *182* (1–3), 64–74.
- (11) Ma, L. M.; Zhang, W. X. Enhanced biological treatment of industrial wastewater with bimetallic zero-valent iron. *Environ. Sci. Technol.* **2008**, *42* (15), 5384–5389.
- (12) Li, A.; Zhao, X.; Hou, Y.; Liu, H.; Wu, L.; Qu, J. The electrocatalytic dechlorination of chloroacetic acids at electrodeposited Pd/Fe-modified carbon paper electrode. *Appl. Catal., B* **2012**, *111*–112 (0), 628–635.
- (13) Wang, X.; Ning, P.; Liu, H.; Ma, J. Dechlorination of chloroacetic acids by Pd/Fe nanoparticles: Effect of drying method on metallic activity and the parameter optimization. *Appl. Catal., B* **2010**, *94* (1–2), 55–63.
- (14) Zhu, N.; Luan, H.; Yuan, S.; Chen, J.; Wu, X.; Wang, L. Effective dechlorination of HCB by nanoscale Cu/Fe particles. *J. Hazard. Mater.* **2010**, *176* (1–3), 1101–1105.
- (15) Hu, C. Y.; Lo, S. L.; Liou, Y. H.; Hsu, Y. W.; Shih, K.; Lin, C. J. Hexavalent chromium removal from near natural water by copper–iron bimetallic particles. *Water Res.* **2010**, *44* (10), 3101–3108.
- (16) Koutsospyros, A.; Pavlov, J.; Fawcett, J.; Strickland, D.; Smolinski, B.; Braida, W. Degradation of high energetic and insensitive munitions compounds by Fe/Cu bimetal reduction. *J. Hazard. Mater.* **2012**, *219*–220, 75–81.
- (17) Bransfield, S. J.; Cwiertny, D. M.; Rorerts, A. L.; Fairbrother, D. H. Influence of copper loading and surface coverage on the reactivity of granular iron toward 1,1,1-trichloroethane. *Environ. Sci. Technol.* **2006**, *40* (5), 1485–1490.
- (18) Bransfield, S. J.; Cwiertny, D. M.; Livi, K.; Fairbrother, D. H. Influence of transition metal additives and temperature on the rate of organohalide reduction by granular iron: Implications for reaction mechanisms. *Appl. Catal., B* **2007**, *76* (3–4), 348–356.
- (19) Cwiertny, D. M.; Bransfield, S. J.; Livi, K. J. T.; Fairbrother, D. H.; Roberts, A. L. Exploring the influence of granular iron additives on 1,1,1-trichloroethane reduction. *Environ. Sci. Technol.* **2006**, *40* (21), 6837–6843.
- (20) Lai, B.; Zhou, Y. X.; Yang, P.; Wang, J. L.; Yang, J. H.; Li, H. Q. Removal of FePO₄ and Fe₃(PO₄)₂ crystals on the surface of passive fillers in Fe⁰/GAC reactor using the acclimated bacteria. *J. Hazard. Mater.* **2012**, *241*–242, 241–51.
- (21) Lai, B.; Zhou, Y. X.; Qin, H. K.; Wu, C. Y.; Pang, C. C.; Lian, Y.; Xu, J. X. Pretreatment of wastewater from acrylonitrile–butadiene–styrene (ABS) resin manufacturing by microelectrolysis. *Chem. Eng. J.* **2012**, *179*, 1–7.
- (22) Coughlin, M. F.; Kinkle, B. K.; Bishop, P. L. Degradation of acid orange 7 in an aerobic biofilm. *Chemosphere* **2002**, *46* (1), 11–19.
- (23) Greenlee, L. F.; Torrey, J. D.; Amaro, R. L.; Shaw, J. M. Kinetics of zero valent iron nanoparticle oxidation in oxygenated water. *Environ. Sci. Technol.* **2012**, *46* (23), 12913–12920.
- (24) Wang, K. S.; Lin, C. L.; Wei, M. C.; Liang, H. H.; Li, H. C.; Chang, C. H.; Fang, Y. T.; Chang, S. H. Effects of dissolved oxygen on dye removal by zero-valent iron. *J. Hazard. Mater.* **2010**, *182* (1–3), 886–95.
- (25) Wang, Z.; Huang, W.; Peng, P. a.; Fennell, D. E. Rapid transformation of 1,2,3,4-TCDD by Pd/Fe catalysts. *Chemosphere* **2010**, *78* (2), 147–151.
- (26) Liu, Y.; Yang, F.; Chen, J.; Gao, L.; Chen, G. Linear free energy relationships for dechlorination of aromatic chlorides by Pd/Fe. *Chemosphere* **2003**, *50* (10), 1275–1279.
- (27) Lin, C. J.; Lo, S. L.; Liou, Y. H. Dechlorination of trichloroethylene in aqueous solution by noble metal-modified iron. *J. Hazard. Mater.* **2004**, *116* (3), 219–28.
- (28) Wang, X. Y.; Chen, C.; Chang, Y.; Liu, H. L. Dechlorination of chlorinated methanes by Pd/Fe bimetallic nanoparticles. *J. Hazard. Mater.* **2009**, *161* (2–3), 815–823.
- (29) Fang, Z. Q.; Qiu, X. H.; Chen, J. H.; Qiu, X. Q. Debromination of polybrominated diphenyl ethers by Ni/Fe bimetallic nanoparticles: Influencing factors, kinetics, and mechanism. *J. Hazard. Mater.* **2011**, *185* (2–3), 958–969.
- (30) Yin, W.; Wu, J.; Li, P.; Wang, X.; Zhu, N.; Wu, P.; Yang, B. Experimental study of zero-valent iron induced nitrobenzene reduction in groundwater: The effects of pH, iron dosage, oxygen and common dissolved anions. *Chem. Eng. J.* **2012**, *184*, 198–204.
- (31) Lai, B.; Chen, Z. Y.; Zhou, Y. X.; Yang, P.; Wang, J. L.; Chen, Z. Q. Removal of high concentration *p*-nitrophenol in aqueous solution by zero valent iron with ultrasonic irradiation (US-ZVI). *J. Hazard. Mater.* **2013**, *250*–251, 220–8.
- (32) Zhang, H.; Duan, L.; Zhang, Y.; Wu, F. The use of ultrasound to enhance the decolorization of the C.I. Acid Orange 7 by zero-valent iron. *Dyes Pigm.* **2005**, *65* (1), 39–43.
- (33) Hung, H. M.; Ling, F. H.; Hoffmann, M. R. Kinetics and mechanism of the enhanced reductive degradation of nitrobenzene by elemental iron in the presence of ultrasound. *Environ. Sci. Technol.* **2000**, *34* (9), 1758–1763.
- (34) Chang, S. H.; Chuang, S. H.; Li, H. C.; Liang, H. H.; Huang, L. C. Comparative study on the degradation of I.C. Remazol Brilliant Blue R and I.C. Acid Black 1 by Fenton oxidation and Fe⁰/air process and toxicity evaluation. *J. Hazard. Mater.* **2009**, *166* (2–3), 1279–88.
- (35) Styliadi, M.; Kondarides, D. I.; Verykios, X. E. Visible light-induced photocatalytic degradation of Acid Orange 7 in aqueous TiO₂ suspensions. *Appl. Catal., B* **2004**, *47* (3), 189–201.
- (36) Feng, W.; Nansheng, D.; Helin, H. Degradation mechanism of azo dye C. I. reactive red 2 by iron powder reduction and photooxidation in aqueous solutions. *Chemosphere* **2000**, *41* (8), 1233–1238.
- (37) Mielczarski, J. A.; Atenas, G. M.; Mielczarski, E. Role of iron surface oxidation layers in decomposition of azo-dye water pollutants in weak acidic solutions. *Appl. Catal., B* **2005**, *56* (4), 289–303.
- (38) Bauer, C.; Jacques, P.; Kalt, A. Investigation of the interaction between a sulfonated azo dye (AO7) and a TiO₂ surface. *Chem. Phys. Lett.* **1999**, *307* (5–6), 397–406.
- (39) Vinodgopal, K.; Wynkoop, D. E.; Kamat, P. V. Environmental photochemistry on semiconductor surfaces: photosensitized degradation of a textile azo dye, Acid Orange 7, on TiO₂ particles using visible light. *Environ. Sci. Technol.* **1996**, *30* (5), 1660–1666.
- (40) Styliadi, M.; Kondarides, D. I.; Verykios, X. E. Pathways of solar light-induced photocatalytic degradation of azo dyes in aqueous TiO₂ suspensions. *Appl. Catal., B* **2003**, *40* (4), 271–286.